

# Schottky Mass-Measurements of Cooled Proton-Rich Nuclei in the Storage Ring ESR

T. Radon<sup>1\*</sup>, Th. Kerscher<sup>2</sup>, B. Schlitt<sup>1</sup>, K. Beckert<sup>1</sup>, T. Beha<sup>2</sup>, F. Bosch<sup>1</sup>, H. Eickhoff<sup>1</sup>, B. Franke<sup>1</sup>, Y. Fujita<sup>3</sup>,  
H. Geissel<sup>1</sup>, M. Hausmann<sup>1</sup>, H. Irnich<sup>1</sup>, H. C. Jung<sup>4</sup>, O. Klepper<sup>1</sup>, H.-J. Kluge<sup>1</sup>, C. Kozhuharov<sup>1</sup>, G. Kraus<sup>1</sup>,  
K. E. G. Löbner<sup>2</sup>, G. Münzenberg<sup>1</sup>, Yu. Novikov<sup>5</sup>, F. Nickel<sup>1</sup>, F. Nolden<sup>1</sup>, Z. Patyk<sup>1</sup>, H. Reich<sup>1</sup>, C. Scheidenberger<sup>1</sup>,  
W. Schwab<sup>1</sup>, M. Steck<sup>1</sup>, K. Sümmerer<sup>1</sup>, H. Wollnik<sup>4</sup>

<sup>1</sup> *Gesellschaft für Schwerionenforschung, Planckstrasse 1, D- 64291 Darmstadt, Germany*

<sup>2</sup> *Sektion Physik, Ludwig-Maximilians-Universität München, Am Coulombwall, D-85748 Garching, Germany*

<sup>3</sup> *College of General Education, Osaka University, Osaka 560, Japan*

<sup>4</sup> *II. Physikalisches Institut, Universität Gießen, Heinrich -Buff-Ring 16, D-35392 Giessen, Germany*

<sup>5</sup> *St. Petersburg Nuclear Physics Institute, Gatchina 188350, Russia*

High-accuracy mass measurements of proton-rich isotopes in the range of  $60 \leq Z \leq 84$  were performed using the novel technique of Schottky spectrometry. Projectile fragments produced by  $^{209}\text{Bi}$  ions at  $930\text{A}\cdot\text{MeV}$  were separated with the magnetic spectrometer FRS and stored and cooled in the storage ring ESR. A typical mass resolving power of 350000 and an accuracy of 100 keV were achieved in the region  $A \approx 200$ . Masses of members of  $\alpha$ -chains linked by precise  $Q_\alpha$  values but not yet connected to the known masses were determined. In this way it is concluded that  $^{201}\text{Fr}$  and  $^{197}\text{At}$  are proton-unbound.

Precise knowledge of atomic masses is required for the understanding of nuclear gross properties and for many applications in other fields of physics, e.g., in astrophysics. In general, masses are well known for nuclei close to  $\beta$  stability, whereas for nuclei far off stability one has mainly to rely on extrapolations. Schottky spectrometry [1,2] of heavy ions at relativistic energies of several hundred  $A\cdot\text{MeV}$  has been used in the present experiment for direct mass measurements of proton-rich nuclides for elements from neodymium to polonium. For lighter nuclei ( $A \leq 58$ ) the potential and power of this new method have been demonstrated before [3,4]. In the case of heavier nuclei, experimental data on masses are especially scarce for refractory elements ( $72 \leq Z \leq 78$ ) because the widely used ISOL-(isotope separator on-line) technique could not access this region. The goals of our experiments were to connect this region of unknown masses to the backbone of known ones, and to measure the members at the end of  $\alpha$ -chains thus providing new information on proton drip line nuclei linked via precise  $Q_\alpha$ -values.

Projectile fragmentation is a powerful and universal tool to access all isotopes with masses smaller than the projectiles. The combination of an in-flight separator for fragments with a storage-cooler ring represents a unique tool for studying exotic nuclei [5]. By merging a cold electron beam with the circulating ions the momentum spread of the cooled ions can be reduced to  $\Delta p/p \leq 10^{-6}$  when the number of stored ions with the same mass-over-charge ratio  $m/q$  is less than  $10^4$  [4,6]. The low momentum spread of stored beams obtained in this way,

---

\*Work done in partial fulfillment of the requirements for the doctor's degree, University of Giessen.

the high sensitivity, as well as the long storage time allow one to perform high-accuracy mass determination. Even single ions circulating in the ring can be observed by detecting its Schottky signal, i.e. the image current induced in pick-up electrodes.

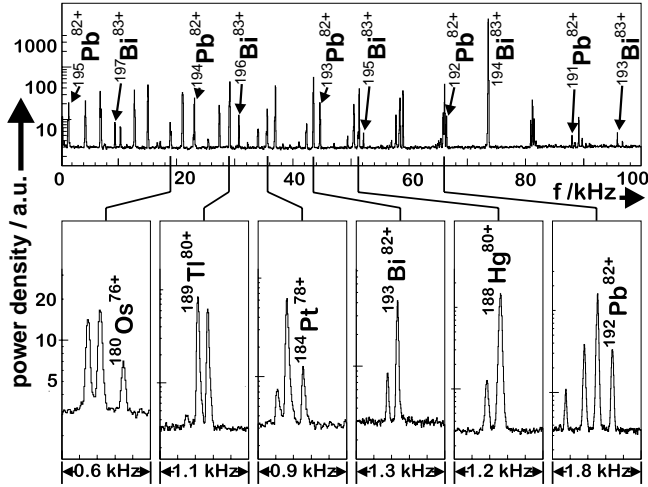


FIG. 1. Schottky frequency spectra for  $^{209}\text{Bi}$ -projectile fragments separated with the FRS and stored and cooled in the ESR. Top: Low-resolution (100 kHz bandwidth) spectrum corresponding to the 16th harmonic of the revolution frequency, which covers nearly the full range of  $m/q$  values (2.5%) for ions accepted inside the ESR. Bottom: High-resolution spectra (10 kHz bandwidth) in which the nuclides under investigation are resolved.

A 930 A·MeV  $^{209}\text{Bi}$ -beam accelerated in the synchrotron SIS is focused on an 8 g/cm<sup>2</sup> beryllium target placed at the entrance of the FRS. Projectile fragments ranging from the proton number of the primary beam down to  $Z=1$  are produced and emerge from the target. Polonium nuclei are generated in the target by proton-pick-up or nuclear charge-changing reactions. The FRS is used as a pure magnetic-rigidity analyzer characterized by an acceptance of  $\Delta(p/q)/(p/q) = \pm 1\%$ , where  $p$  denotes the momentum of an ion. For the selected thickness of the target mainly bare, H-like, and He-like ions emerge, and since the energy loss in this thick target is drastically different for the different elements, their range is restricted to atomic numbers between  $Z=60$  and 84 after separation by the FRS. Several field settings of the FRS are applied each transmitting a different  $p/q$ -band. The separated projectile fragments with mean kinetic energies of about 350 A·MeV are injected into the ESR where they are stored and electron cooled to an identical mean velocity determined by the velocity of the cooler electrons. In this case the revolution frequency of each ion is defined by its mass-to-charge ratio which is the basis for Schottky Mass Spectrometry (SMS). The stored ions circulate in the ESR (circumference  $\approx 108$  m) with frequencies

of about 1.9 MHz. The Schottky signal induced in a pick-up probe is recorded for about 150 msec and subsequently frequency analyzed by Fast-Fourier Transformation (FFT). Mixing with 30 MHz transforms the spectrum of the 16<sup>th</sup> harmonic of the revolution frequency to the 100 kHz bandwidth of the frequency analyzer. A high signal-to-noise ratio is obtained by averaging up to 10<sup>4</sup> single FFT-spectra which yields a measuring time to of roughly roughly 3 min. Figure 1 shows an example of a Schottky spectrum with 100 kHz bandwidth almost covering the ESR  $m/q$ -acceptance of 2.5 %. In this case the magnetic rigidity of the FRS is set to optimize the transmission of fully-ionized <sup>197</sup>Bi fragments. The spectrum consists of the Schottky signals of about 60 ion species (30 nuclei in up to three charge states: bare, H-like, He-like). However they cannot be resolved in 100 kHz overview spectra. An increased frequency resolution is obtained for the 10 kHz spectra mode of the frequency analyzer (Fig 1).

Due to the large amount of peaks, the assignment of the different peaks to isotope and charge state represents a major step in the evaluation process. The observed frequency peaks are related to mass values by

$$\frac{\Delta f}{f} = -\alpha_p \frac{\Delta(m/q)}{(m/q)} \quad (1)$$

where  $f$  is the mean revolution frequency of the ion species and  $(m/q)$  is the corresponding mass-to-charge ratio.  $\Delta f$  is the difference of the frequencies corresponding to the considered  $\Delta(m/q)$  value either for calibration or mass evaluation. The momentum compaction factor  $\alpha_p$  depends on the ion optical operation mode of the ESR and denotes the ratio of the relative change in path length per turn to the relative change of the corresponding magnetic rigidity.

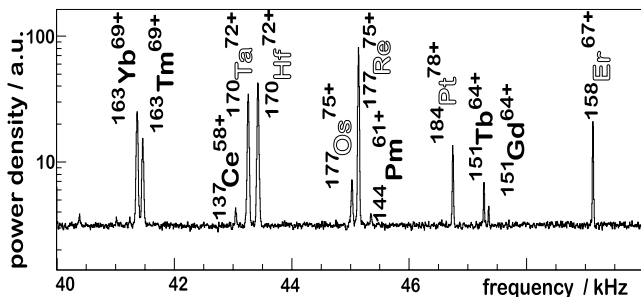


FIG. 2. High resolution Schottky spectrum (10 kHz bandwidth) for the mass determination of <sup>184</sup>Pt. The peaks of ions with known masses used for calibration are indicated by bold letters, nuclei with previously unknown masses by outlined letters. Note that mother and daughter nuclei connected by a  $\beta$ -decay chain are shown in the spectra as close lying mass doublets. For the isobaric pairs of <sup>177</sup>Os<sup>75+</sup> (H-like) and <sup>177</sup>Re<sup>75+</sup> (bare) or <sup>170</sup>Ta<sup>72+</sup> (H-like) and <sup>170</sup>Hf<sup>72+</sup> (bare) the  $Q_\beta$  values were not known.

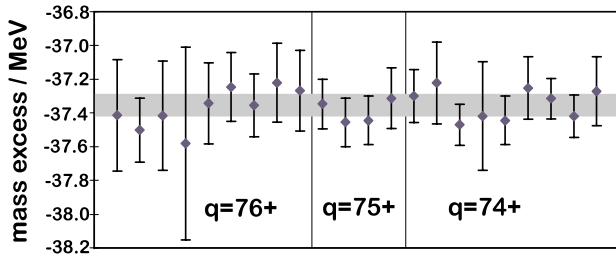


FIG. 3. Mass excess for  $^{184}\text{Pt}$  as determined in several runs using different reference isotopes and in different ionic charge states  $q$ . The shaded area shows the statistical error band after averaging.

For the purpose of peak identification mass values taken from ref. [8] and corrected for the missing electrons and their respective binding energies [9–11] allow one to compute the frequency differences for all tabulated nuclides in different charge states. The calculated frequency spectra exhibit a characteristic pattern and enable a computer assisted pattern recognition of mass spectra. This leads to an unambiguous assignment of mass number, atomic number, and charge state. After this identification procedure the spectra recorded with a smaller detection bandwidth of 10 kHz are used for mass determination. The mass value of the ion under investigation, e. g.  $^{184}\text{Pt}$ , can be determined by comparing its revolution frequency to those of ions with known mass values. As an example, Fig. 2 shows a high resolution spectrum taken with a  $p/q$ -setting of the FRS different from that of Fig. 1. It contains six isotopes with unknown masses and another six with known masses. Each peak is fitted with a Gaussian and a linear background. The momentum compaction factor ( $\alpha_p \approx 0.14$ ) is calibrated according to (1) using neighbouring peaks of isotopes with known masses. Over the full range of a 100 kHz spectrum deviations of the order of 1% are observed for  $\alpha_p$ . This can be caused by inhomogeneities and instabilities of the magnetic fields of the ESR. Therefore, the  $\alpha_p$ -calibration is restricted to a smaller portion of the frequency spectrum in the neighbourhood of the masses of interest. With  $\alpha_p$  determined in this way new mass values can be assigned using several reference peaks.

TABLE I. Mass values in units of  $u$  determined in this experiment\* compared with extrapolations given in Ref. [8] $^\circ$ .

| Nuclide           | Mass (u)*     | Mass (u) $^\circ$ |
|-------------------|---------------|-------------------|
| $^{180}\text{Os}$ | 179.95240(10) | 179.95236(19)     |
| $^{184}\text{Pt}$ | 183.95991(9)  | 183.95989(19)     |
| $^{188}\text{Hg}$ | 187.96753(10) | 187.96755(19)     |
| $^{192}\text{Pb}$ | 191.97579(15) | 191.97576(19)     |
| $^{189}\text{Tl}$ | 188.97391(9)  | 188.97369(38)     |
| $^{193}\text{Bi}$ | 192.98304(15) | 192.98306(38)     |

An important feature of the SMS-method is the possibility to use a large number of well-known masses for an accurate calibration. For example, the signals of stable or long-lived isotopes like H-like  $^{151}\text{Tb}$  and bare  $^{144}\text{Pm}$  are used for the calibration for nuclei far from stability, like bare  $^{184}\text{Pt}$ . Even more, since most of the ions are measured in three different ionic charge states thus appearing in several spectra surrounded by different reference nuclides, redundant and independent mass determinations are possible. As an example for this important feature the mass measurement of  $^{184}\text{Pt}$  is illustrated in Fig. 3. The shaded area represents the weighted average error-band of the data points. With SMS we achieve a high resolving power of  $m/\Delta m$  (*FWHM*)  $\approx 350000$ , and an accuracy of  $\delta m/m \approx 5 \cdot 10^{-7}$  corresponding to about 100 keV.

The uncertainties of statistical origin in the mass evaluation of the present experiment result from the determination of the revolution frequencies. The frequencies of the 16<sup>th</sup> harmonic of about  $f = 30$  MHz are determined with an accuracy of about  $\pm 1$  Hz, i. e., with a relative uncertainty of  $\delta f/f \simeq \pm 3 \cdot 10^{-8}$ . The width (FWHM) of the peaks corresponds to approximately 500 keV. The uncertainties of the known mass values used for calibration range from a few 10 keV to 200 keV [8] and are taken care of as well.

The non-linearity of  $\alpha_p$  causes a systematic error. As we cannot precisely determine the global slope of the  $\alpha_p$  as a function of  $m/q$  for the full acceptance of the ESR, we restrict ourselves to calibrating small frequency ranges only. A comparison of our multiple and independent direct measurements with only known masses from Ref. [8] results in a normal distribution around zero but shows that we have to increase the statistical error by about 80 keV. Representative results are shown in Table I. These nuclei are members of the two  $\alpha$ -decay chains starting at  $^{201}\text{Fr}$  and  $^{200}\text{Rn}$  (Fig. 4). Their mass values are compared with extrapolations given in Ref. [8].

The insert of Fig. 4 shows a comparison of  $Q_\alpha$  values deduced from the directly measured masses in this experiment with the precise  $Q_\alpha$  values from the literature [12–16]. Both data agree within the error bars which are dominated by the SMS-results due to the small uncertainties of the  $Q_\alpha$  values (5–20 keV). Using the SMS-data from Table I and the  $Q_\alpha$  values from [12–16] as shown in Fig. 4 the masses for the short-lived nuclei  $^{196}\text{Po}$ ,  $^{197}\text{At}$ ,  $^{200}\text{Rn}$  and  $^{201}\text{Fr}$  were determined.

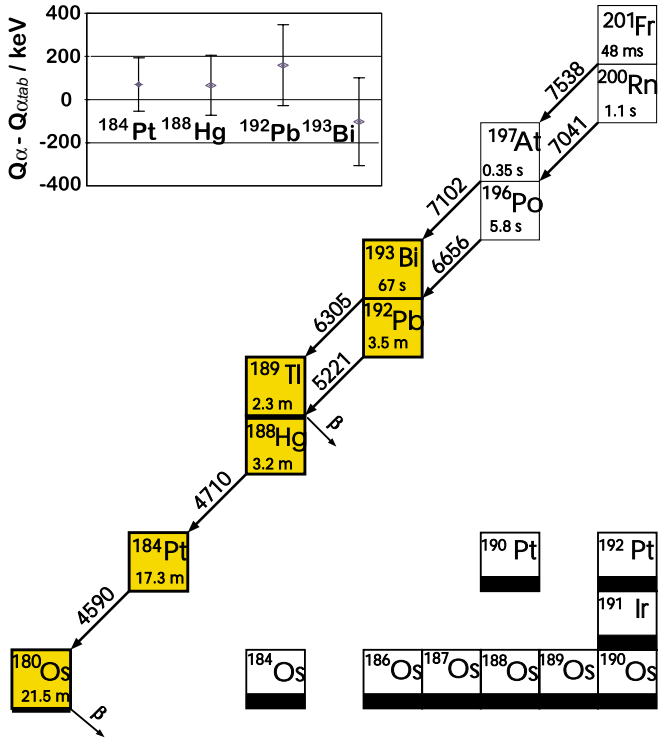


FIG. 4. Two  $\alpha$ -decay chains for which six mass values are determined by SMS in the present work (shaded boxes). The half-lives and the  $Q_\alpha$  values (keV) are indicated. Stable isotopes of platinum, iridium and osmium are shown for orientation. The insert shows a comparison between directly determined  $Q_{\alpha\ tab}$  values and those for SMS (Table I).

The accuracy for the masses of  $^{196}\text{Po}$  and  $^{200}\text{Rn}$  is significantly improved by using the different directly measured masses of the members of the same  $\alpha$ -chain, like  $^{180}\text{Os}$ ,  $^{184}\text{Pt}$ ,  $^{188}\text{Hg}$ ,  $^{192}\text{Pb}$ , in addition to the  $Q_\alpha$  values. The results are listed in Table II. In the same way the masses are determined for the odd-proton nuclides  $^{197}\text{At}$  and  $^{201}\text{Fr}$ .

TABLE II. Mass values for the short-lived nuclei at the top of the  $\alpha$  chain (see Fig. 4) obtained by using our SMS mass values\* and  $Q_\alpha$ -values from Ref. [12–16] compared to extrapolations given in Ref. [8].<sup>◊</sup>

| nuclide           | Mass (u)*     | Mass (u) <sup>◊</sup> |
|-------------------|---------------|-----------------------|
| $^{196}\text{Po}$ | 195.98552(5)  | 195.98551(19)         |
| $^{200}\text{Rn}$ | 199.99568(5)  | 199.99568(19)         |
| $^{197}\text{At}$ | 196.99346(8)  | 196.99329(38)         |
| $^{201}\text{Fr}$ | 201.00416(10) | 201.00399(38)         |

Proton separation energies and pairing energies are of fundamental interest for the theoretical description of exotic nuclei [17]. Using the experimental mass values one can derive the proton separation energies

$$S_p(Z, A) = m(Z - 1, A - 1) + m_H - m(Z, A).$$

For  $^{201}\text{Fr}$  and  $^{197}\text{At}$ , at the top of the  $\alpha$ -chain displayed in Fig. 4, we obtain

$$S_p(^{201}\text{Fr}) = -(570 \pm 110) \text{ keV}$$

$$S_p(^{197}\text{At}) = -(80 \pm 80) \text{ keV}$$

i.e., both nuclei are proton-unbound. The proton separation energies are compared to different global calculations, as Extended Thomas-Fermi [18], Thomas-Fermi [19] and macroscopic-microscopic [20] models. These models yield for  $^{201}\text{Fr}$  279 keV [18], -1 keV [19], 79 keV [20] and for  $^{197}\text{At}$  379 keV [18], 189 keV [19], 259 keV [20], respectively. In agreement with the experiment all models give a smaller value for the proton separation energy for  $^{201}\text{Fr}$  than for  $^{197}\text{At}$ . The property of being proton-unbound does not necessarily mean that such nuclei are proton emitters, e.g., a rough estimate for the penetrability of protons through the Coulomb barrier of  $^{201}\text{Fr}$  [21] yields a proton partial half-life of  $T_{1/2}(p) \approx 10^8\text{s}$ . This means a proton emission from the ground state is very unlikely. The heaviest known proton emitter in this mass region is  $^{185}\text{Bi}$  [22].

The results presented in this Letter were selected to demonstrate the power of Schottky spectrometry in combination with the FRS-ESR system for mass measurements. In a run of a few days the masses of more than 280 isotopes have been determined. We succeeded to measure about hundred previously unknown or not accepted mass values [23,24]. These results will be published elsewhere. Electron cooling of highly charged ions confined in a storage ring enables high-accuracy mass spectrometry via detecting the Schottky signal. We obtained in this experiment a resolving power for heavy nuclei as high as  $m/\delta m$  (FWHM)  $\approx 350000$  and the overall uncertainties of the mass determination are in the range from 80 to 200 keV and reach 50 keV in case of known  $Q_\alpha$  values. The excellent sensitivity of SMS allows that even a single ion circulating in the ESR can be detected [25]. Unstable nuclides can be measured if their lifetime exceeds the time required for cooling and frequency analysis, which was of the order of one minute.

It should be noted that mother and daughter nuclei connected by a  $\beta$ -decay chain are often observed in the Schottky spectrum as close lying mass multiplets. SMS provides therefore not only direct mass spectrometry of nuclei far from stability but also a new approach for  $Q_\beta$ -measurements of exotic nuclides.

The authors would like to thank the GSI staff for excellent support during the experiments. This work has been

financially supported by the German Federal Minister for Education, Science, Research, and Technology (BMBF) under contract number 06 LM 363 and the Beschleunigerlaboratorium München.

---

- [1] B. Franzke *et al.*, Phys. Scripta **T59**, 176 (1995).
- [2] B. Schlitt *et al.*, Hyp. Int. **99**, 117 (1996).
- [3] H. Geissel *et al.*, Phys. Rev. Lett. **68**, 3412 (1992).
- [4] H. Irnich *et al.*, Phys. Rev. Lett. **75**, 4182 (1995).
- [5] H. Geissel, G. Münzenberg, K. Riisager, Ann. Rev. Nucl. Part. Sci. **45**, 163 (1995).
- [6] M. Steck *et al.*, Hyp. Int. **99**, 245 (1996).
- [7] H. Geissel *et al.*, Nucl. Instr. Meth. **B70**, 286 (1992).
- [8] G. Audi and A. H. Wapstra, Nucl. Phys. **565**, 66 (1993) and Nucl. Phys. **595** 409 (1995).
- [9] K. N. Huang *et al.*, At. Data Nucl. Data Tables **18**, 243 (1976).
- [10] W. R. Johnson and G. Soff, At. Data Nucl. Data Tables **39**, 265 (1988).
- [11] D. R. Plante, W. R. Johnson, J. Sapirstein, Phys. Rev. **A49**, 3519 (1994).
- [12] A. Rytz, At. Data Nucl. Data Tables **47**, 205 (1991).
- [13] B. Buck, A. C. Merchant and S. M. Perez, At. Data Nucl. Data Tables **54**, 53 (1993).
- [14] E. Coenen *et al.*, Phys. Rev. Lett., **54**, 1783 (1985) and Proc. AMCO-7 conference Darmstadt p.272 (1984).
- [15] T. Enquist *et al.*, Z. Phys **A354**, 1 (1996).
- [16] Zhou Chunmei, NDS **76**, 399 (1995).
- [17] R. Smolańczuk and J. Dobaczewski, Phys. Rev. C **48**, R2166 (1993).
- [18] Y. Aboussir *et al.*, Nucl. Phys. **A549**,155 (1992).
- [19] W.D. Myers and W.J. Swiatecki, Nucl. Phys. **A601**,141 (1996).
- [20] P. Moeller *et al.*, At. Data Nucl. Data Tables **59**,185 (1995).
- [21] V. I. Goldanskii, Ann. Rev. Nucl. Sci. **16**, 1 (1966).
- [22] C.N. Davids *et al.*, ENAM'95 conference, Arles, (1995).
- [23] T. Beha, Thesis, LMU München (1995).
- [24] Th. Kerscher, Thesis, LMU München (1996).
- [25] B. Franzke *et al.*, GSI Scientific Report **GSI-96-1**,159 (1996).